is simplified if we remember that each member in the pair of sequences 6 and 9, 12 and 15, 18 and 21, etc. leads to the loss of the same number of spins, namely, in order, 2, 4, 6, and so on. We find then, that 26–30% of the original, magnetically active Ti^{3+} sequences will become magnetically inactive, given removal of 12–15% of the $AlCl_3$ from β-$(TiCl_3)(AlCl_3)_{0.33}$. On the basis of this scenario, the spins per titanium now expected for structure IV would be suppressed to only 0.23–0.24. Once again structure IV, modified for contribution from this crystalline impurity, yields the best agreement with experiment from among the four structures considered.

On the other hand, as we mentioned, the impurity could also be γ-$(TiCl_3)(AlCl_3)_{0.33}$. This phase of the cocrystallized $TiCl_3$ and $AlCl_3$ has a layer-lattice structure and, at room temperature, gives 1 spin/Ti^{3+}.[15] If 4% of the material examined is in the γ-phase, then the effect will be to raise the spin/Ti^{3+} value for any of the sequence distribution structures I–IV by 0.02–0.03. This being the case, the best fit with experiment again is clearly obtained with sequence distribution structure IV.

After consideration of all the sequence distribution structures, and the effects of chain lengths and impurities on the experimental results, we conclude that only structure IV is consistent with these results.

Conclusion

For the first time, the sequence distribution concepts originally applied for detailed understanding of organic copolymer microstructure have been used to interpret the magnetic behavior of an inorganic copolymer, β-$(TiCl_3)(AlCl_3)_{0.33}$. The magnetic properties are best matched by using a sequence distribution model consisting of fixed, alternating runs of Al^{3+} ions and Ti^{3+} ions of lengths one and three, respectively. This newly gained sequence distribution information can provide insight into the growth mechanism for such chains, a subject we intend to discuss in a forthcoming paper.

Acknowledgment. Discussions with Dr. Jim Randall and the comments of Dr. David Johnston are gratefully acknowledged. The authors thank Exxon Chemical Co. for permission to publish this work.

Registry No. $TiCl_3$, 7705-07-9; $AlCl_3$, 7446-70-0.

Contribution from the Department of Chemistry, University of Tennessee, Knoxville, Tennessee 37996-1600, and Transuranium Research Laboratory (Chemistry Division), Oak Ridge National Laboratory, Oak Ridge, Tennessee 37831

Absorption Spectrophotometric and X-ray Diffraction Studies of the Trichlorides of Berkelium-249 and Californium-249[1a]

J. R. Peterson,*[1b] J. P. Young,[1c] D. D. Ensor,[1d] and R. G. Haire[1c]

Received April 9, 1986

Absorption spectrophotometric and X-ray powder diffraction methods have been applied to a study of the trichlorides of ^{249}Bk and ^{249}Cf and their relationship through the β decay of ^{249}Bk. $BkCl_3$ has been prepared for the first time in the $PuBr_3$-type orthorhombic modification by quenching from the melt. Each of the crystal forms (UCl_3-type hexagonal and $PuBr_3$-type orthorhombic) of $BkCl_3$ and $CfCl_3$ has been characterized on the basis of its solid-state absorption spectrum. The orthorhombic forms of $BkCl_3$ and $CfCl_3$ are the high-temperature modifications with respect to the hexagonal phases, with the apparent transition temperatures near the melting points of $BkCl_3$ (876 K) and $CfCl_3$ (818 K). Orthorhombic $BkCl_3$ transmutes to orthorhombic $CfCl_3$ and hexagonal $BkCl_3$ transmutes to hexagonal $CfCl_3$. Thus, it was found that both the oxidation state and the crystal structure of the parent ^{249}Bk compound were retained by the daughter ^{249}Cf compound through β decay in the bulk phase solid state.

Introduction

The first preparations of berkelium trichloride and californium trichloride were reported almost 20 years ago.[2,3] From the analysis of X-ray powder diffraction data, both compounds were found to exhibit the UCl_3-type hexagonal structure. Their average, room-temperature lattice parameters were determined to be a_0 = 0.7382 (2) nm and c_0 = 0.4127 (3) nm for $BkCl_3$[2] and a_0 = 0.7393 (40) nm and c_0 = 0.4090 (60) nm for $CfCl_3$.[3] In each case a list of observed and calculated diffraction lines was presented along with a comparison of the observed and calculated intensities of the diffraction lines. Comparison of the similarly calculated trivalent ionic radii of the lanthanides and actinides that exhibit the UCl_3-type hexagonal structure and the fact that the crystal structure of the lanthanide trichlorides changes between gadolinium (UCl_3-type hexagonal) and terbium ($PuBr_3$-type orthorhombic) led to the prediction that a crystal structure change should occur in the actinide trichlorides heavier than $CfCl_3$.[2]

Single crystals of californium trichloride were grown from the melt on the microgram scale and used to establish the existence of the $PuBr_3$-type orthorhombic phase (o-$CfCl_3$) for this compound, as well as to refine the structures of both the known UCl_3-type hexagonal phase (h-$CfCl_3$) and this newly discovered orthorhombic phase.[4] The room-temperature lattice parameters determined from the single crystal of each form were a_0 = 0.7379 (1) nm and c_0 = 0.40900 (5) nm for h-$CfCl_3$ and a_0 = 0.3869 (2), b_0 = 1.1748 (7), and c_0 = 0.8561 (4) nm for o-$CfCl_3$. Although the melting point of $CfCl_3$ was established as 818 ± 5 K, the temperature relationship between the hexagonal and orthorhombic phases could not be determined.[4]

In the present work we have utilized a microscope–spectrophotometer of local design to obtain solid-state absorption spectra from microgram-sized samples of $BkCl_3$ and $CfCl_3$. We have (1) prepared $BkCl_3$ in the previously unknown $PuBr_3$-type orthorhombic modification (o-$BkCl_3$), (2) characterized spectrophotometrically the orthorhombic and hexagonal forms of both $BkCl_3$ and $CfCl_3$, (3) determined the chemical and physical consequences of the β decay of both crystal forms of $^{249}BkCl_3$, and (4) deter-

(1) (a) Research sponsored by the Division of Chemical Sciences, U.S. Department of Energy, under Contracts DE-AS05-76ER04447 with the University of Tennessee, Knoxville, TN, and DE-AC05-84OR21400 with Martin Marietta Energy Systems, Inc. (b) University of Tennessee. (c) Oak Ridge National Laboratory. (d) Department of Chemistry, Tennessee Technological University, Cookeville, TN 38505.
(2) Peterson, J. R.; Cunningham, B. B. *J. Inorg. Nucl. Chem.* **1968**, *30*, 823.
(3) Green, J. L.; Cunningham, B. B. *Inorg. Nucl. Chem. Lett.* **1967**, *3*, 343.
(4) Burns, J. H.; Peterson, J. R.; Baybarz, R. D. *J. Inorg. Nucl. Chem.* **1973**, *35*, 1171.

0020-1669/86/1325-3779$01.50/0

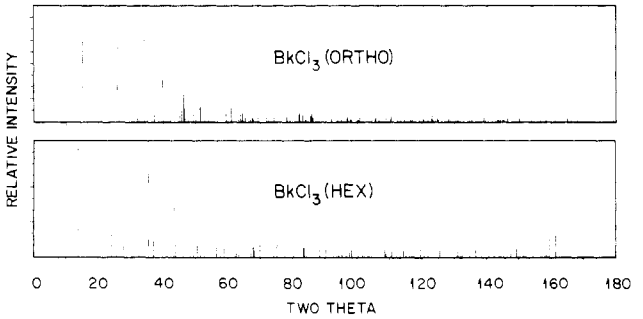

Figure 1. Theoretical powder diffraction patterns of hexagonal and orthorhombic $BkCl_3$.

mined the temperature relationship between the hexagonal (denoted *h*) and orthorhombic (denoted *o*) crystal structures of $BkCl_3$ and $CfCl_3$.

Experimental Section

Materials. The ^{249}Bk ($T_{1/2}$ = 320 days; β emitter) was synthesized in the High Flux Isotope Reactor (HFIR) at the Oak Ridge National Laboratory. Californium-249 ($T_{1/2}$ = 351 years; α emitter) is produced isotopically pure by the β decay of ^{249}Bk. The source Bk(III) and Cf(III) were separated and purified by standard solvent extraction and/or ion-exchange methods.[5]

Sample Preparation. The microscale chemical procedures used to prepare samples of $BkCl_3$ and $CfCl_3$ of 1–10-μg mass are summarized elsewhere.[6] For completeness we detail the preparative chemistry in reaction equation format, with An representing Bk or Cf:

$$2An^{3+}(aq) + 3C_2O_4^{2-}(aq) \rightarrow An_2(C_2O_4)_3(s) \quad (1)$$

$$An_2(C_2O_4)_3(s) + (2 - x)O_2(g) \xrightarrow{1300\ K} 2AnO_{2-x}(s) + 6CO_2 \quad (2)$$

$$2AnO_{2-x}(s) + 6HCl(g) \xrightarrow{>725\ K} 2AnCl_3(s) + 3H_2O(g) + (^1/_2 - x)O_2 \quad (3)$$

The microprecipitation (eq 1) was carried out with 20–30-μg masses of An^{3+} in a conical Teflon form. The calcination (eq 2) in oxygen (or air) was performed in an oven with the solid oxalate chunk(s) in a platinum boat. Pieces (1–10 μg) of the oxide product were transferred to individual fused silica capillaries that attached to our synthesis system.[6] The hydrochlorination (eq 3) took place in situ. The chlorides were encapsulated under 76 kPa of HCl(g) by flame sealing the fused silica capillaries and were then characterized both by X-ray powder diffraction and absorption spectrophotometric analysis.

Phase changes, from hexagonal to orthorhombic and from orthorhombic to hexagonal, were brought about by heating (and subsequently cooling) a chloride sample in situ by means of a resistively heated platinum-wire coil located externally to and coaxially with the sample-containing capillary.

Sample Characterization. The encapsulated trichloride samples were examined by both absorption spectrophotometry and X-ray powder diffraction. Solid-state absorption spectra were obtained from the sample at room temperature over the wavelength range 320–1100 nm. Our microscope–spectrophotometer is a single-beam instrument; it and the data-handling procedures are described elsewhere.[6] The techniques we employ to obtain X-ray powder diffraction patterns from actinide compounds have also been published.[7] Trichloride samples that had been melted often yielded spotty diffraction patterns indicative of macrocrystallites. Such samples, however, are ideally suited for optical transmission spectroscopy. Theoretical X-ray diffraction powder patterns were computer-generated by using the program POWD.[8]

Results and Discussion

Samples of $BkCl_3$ and $CfCl_3$ prepared at ~775 K exhibited the UCl_3-type hexagonal structure as confirmed by the analysis of X-ray powder diffraction data. Theoretical powder diffraction patterns of both crystal forms of $BkCl_3$, calculated by using the atomic coordinates of $CfCl_3$[4] and including no correction for sample absorption, are given in Figure 1. Confirmation of the hexagonal structure for $BkCl_3$ was based on the presence of the four strong diffraction lines [angle (*hkl*)] at 2θ (λ = 0.154 178 nm) = 13.8 (100), 24.1 (110), 35.5 (201), and 43.4° (211) and the concomitant absence of the characteristic diffraction lines of the $PuBr_3$-type orthorhombic structure at 2θ (λ = 0.154 178 nm) = 15.1 (020), 20.7 (002), 26.2 (111), 34.1 (131), and 39.9° (113). The corresponding angles (*hkl*) for *h*-$CfCl_3$ are 13.9 (100), 24.1 (110), 35.7 (201), and 43.5° (211) and for *o*-$CfCl_3$ are 15.1 (020), 20.8 (002), 26.4 (111), 34.2 (131), and 40.0° (113).

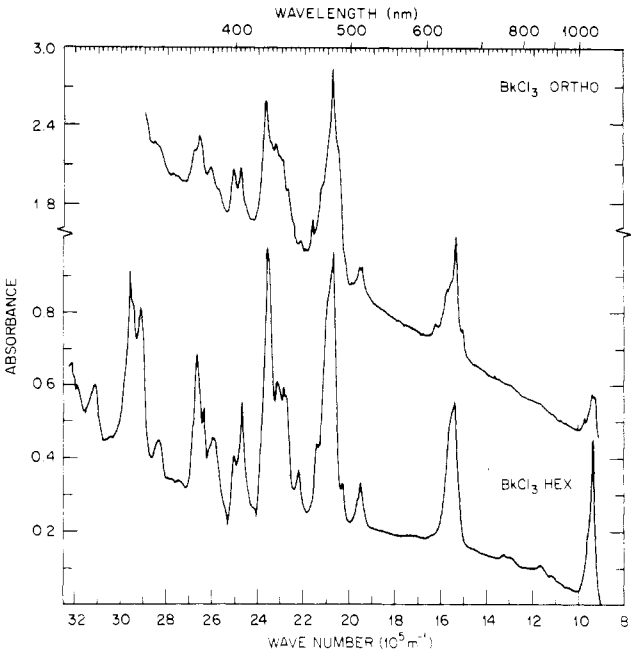

Figure 2. Absorption spectra of hexagonal and orthorhombic $BkCl_3$ at room temperature.

The orthorhombic form of the trichlorides was prepared by quenching from the melt. Confirmation of this structure was achieved by analysis of the X-ray diffraction data. In earlier work on dimorphic $CfCl_3$,[4] the temperature relationship of the two crystallographic modifications could not be determined. A report of similar dimorphism in $GdCl_3$ concluded that *o*-$GdCl_3$ is the low-temperature form with a transition (to *h*-$GdCl_3$) temperature of about 373 K.[9] In contrast, the results of our thermal annealing and quenching studies indicate that both *o*-$BkCl_3$ and *o*-$CfCl_3$ are the high-temperature forms with phase transition (to the respective hexagonal forms) temperatures close to their melting points, 876[10] and 818 K,[4] respectively. Further work is necessary to describe in greater detail the precise conditions of the hexagonal ↔ orthorhombic phase transformations.

Room-temperature solid-state absorption spectra of X-ray-confirmed *h*-$BkCl_3$ and *o*-$BkCl_3$ are presented in Figure 2. The absorption peaks result from the Laporte forbidden f–f transitions in the Bk(III) ions. *h*-$BkCl_3$ is identified, for example, on the basis of the sharp peaks at 9.3 × 10^5 and 19.5 × 10^5 m^{-1}, in contrast to their truncated counterparts in *o*-$BkCl_3$, the differing absorption band shapes at 15.4 × 10^5 m^{-1} (less fine structure in *h*-$BkCl_3$), at 20.8 × 10^5 m^{-1}, between 22.7 × 10^5 and 23.8 × 10^5 m^{-1}, and around 25 × 10^5 m^{-1} (asymmetric doublet in *h*-$BkCl_3$ vs. a symmetric one in *o*-$BkCl_3$). Visual examination of these and/or other spectral features of an absorption spectrum of $BkCl_3$ and comparison to those presented in Figure 2 are usually sufficient to identify with certainty the crystal form exhibited by the $BkCl_3$ sample. If the $BkCl_3$ sample contains as little as 5% $CfCl_3$, then the determination of the crystal structure of the parent $BkCl_3$

(5) Baybarz, R. D.; Knauer, J. B.; Orr, P. B. Union Carbide Corp., Oak Ridge National Laboratory, U.S. Atomic Energy Commission Document ORNL-4672, 1973.
(6) Young, J. P.; Haire, R. G.; Fellows, R. L.; Peterson, J. R. *J. Radioanal. Chem.* **1978**, *43*, 479.
(7) Peterson, J. R. *Advances in X-Ray Analysis*; McMurdie, H. F., Barrett, C. S.; Newkirk, J. B., Ruud, C. O., Eds.; Plenum: New York, 1977; Vol. 20, p 75.
(8) Smith, D. K. University of California, Lawrence Radiation Laboratory, U.S. Atomic Energy Commission Document UCRL-7196, 1963.
(9) Harris, A. L.; Veale, C. R. *J. Inorg. Nucl. Chem.* **1965**, *27*, 1437.
(10) Peterson, J. R.; Burns, J. H. *J. Inorg. Nucl. Chem.* **1973**, *35*, 1525.

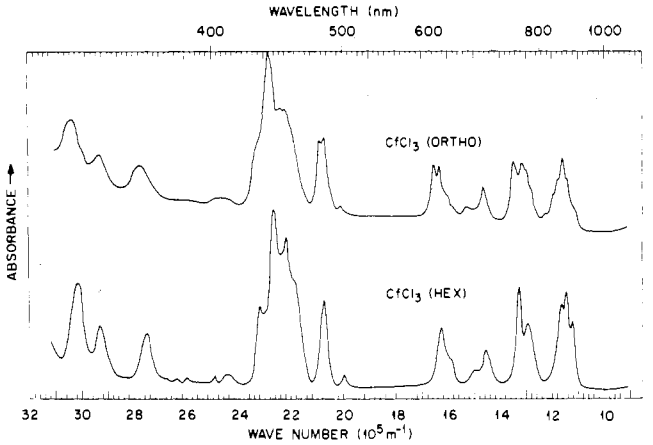

Figure 3. Absorption spectra of hexagonal and orthorhombic $CfCl_3$ at room temperature.

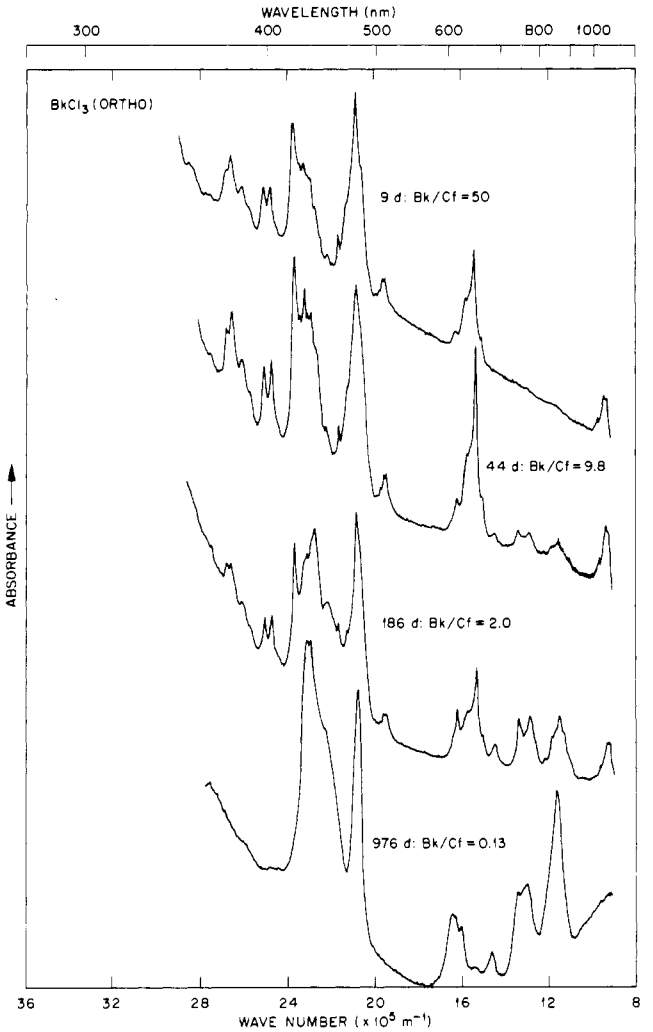

Figure 4. Absorption spectra of orthorhombic $BkCl_3$ as a function of time. (The 976 d spectrum suffers from instrumental artifacts that result in altered absorption intensities.)

sample can be based on the character of the Cf(III) absorption bands at about 11.4×10^5 and 13×10^5 m^{-1}, as discussed next.

Room-temperature solid-state absorption spectra of X-ray-confirmed *h*-$CfCl_3$ and *o*-$CfCl_3$ are given in Figure 3. They are easily distinguished by the different shapes of the f–f absorption bands at about 11.4×10^5, 13×10^5 and 16.2×10^5 m^{-1}. For example, the absorption bands at about 11.4×10^5 and 13×10^5 m^{-1} are relatively more symmetrical in *o*-$CfCl_3$ and more asymmetrical in *h*-$CfCl_3$; the absorption peak at about 16.2×10^5 m^{-1} is split in *o*-$CfCl_3$ and unsplit in *h*-$CfCl_3$. These and other differences between the absorption spectra of the two crystal forms of $CfCl_3$ are reproducible and used to identify which crystal structure is exhibited by a particular sample of $CfCl_3$.

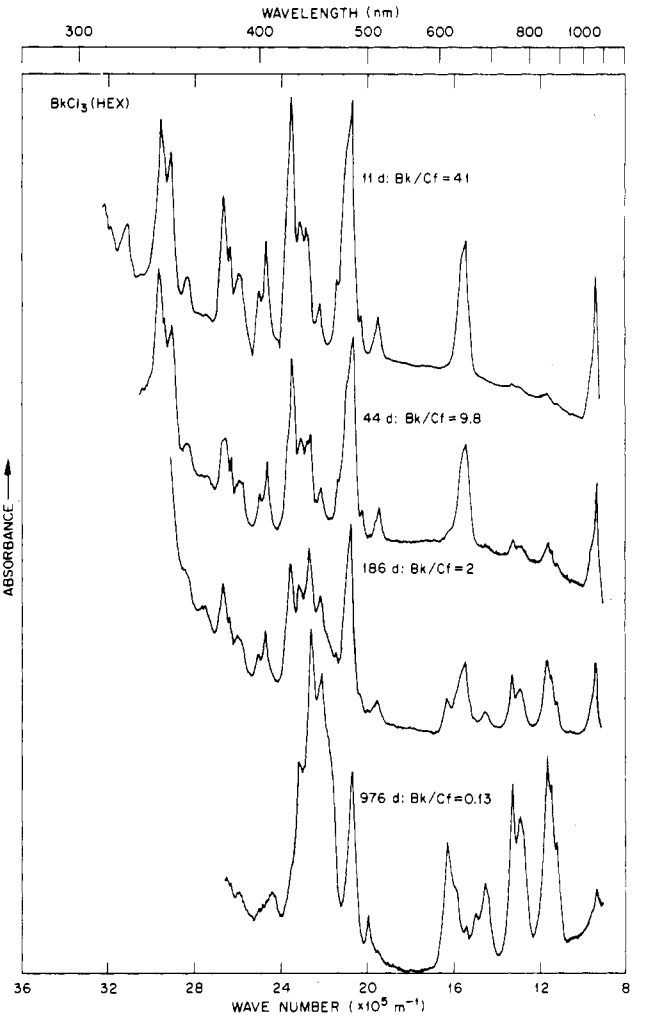

Figure 5. Absorption spectra of hexagonal $BkCl_3$ as a function of time.

The chemical and physical consequences of the β decay of $BkCl_3$ were determined from the interpretation of absorption spectra obtained from a sample of *h*-$BkCl_3$ and from a sample of *o*-$BkCl_3$ over a period of several years. In Figure 4 are given four absorption spectra of *o*-$BkCl_3$, taken at 9, 44, 186, and 976 days after the initial separation of parent Bk and daughter Cf. The spectrum growing into this *o*-$BkCl_3$ matches that of *o*-$CfCl_3$ in Figure 3. In the case of *h*-$BkCl_3$ (see Figure 5; spectra taken at 11, 44, 186, and 976 days after the Bk–Cf separation), the absorption spectrum of the ingrown Cf(III) matches that of *h*-$CfCl_3$ in Figure 3. Note that in both cases the absorption spectrum taken at 44 days (ca. 9% Cf) already reveals at 11.4×10^5 and 13×10^5 m^{-1} the absorption peaks of Cf(III) exhibiting the characteristics generally used to differentiate between the two trichloride crystal structures. In most of the $BkCl_3$ samples whose absorption spectra we have monitored over time, the crystal structure exhibited by the ingrowing $CfCl_3$ has been spectrophotometrically identified by the time of the Cf composition is about 5%, that is, within about 23 days from the Bk–Cf separation. In both studies over time the aged $BkCl_3$ samples were also examined by X-ray powder diffraction to confirm that the structure of the ingrown $CfCl_3$ was indeed the same as that of the parent $BkCl_3$ sample. Thus, two investigative methods have shown that the trivalent oxidation state and both the local and long-range structures of the Bk ions are retained by the Cf ions resulting from β decay in the bulk phase solid state. The maintenance of oxidation state, a chemical consequence of the β decay, means that following the emission of a beta particle ($^0_{-1}e^-$) from the Bk nucleus, $^{249}_{97}Bk^{3+} \rightarrow {}^{249}_{98}Cf^{4+} + {}^0_{-1}e^-$, a rearrangement of electronic charge occurs to yield

$^{249}_{98}Cf^{3+}$, that is $^{249}_{98}Cf^{4+} + {}^{0}_{-1}e^{-} \rightarrow {}^{249}_{98}Cf^{3+}$. The necessity to maintain overall electroneutrality in the trichloride sample favors the maintenance of metal ion oxidation state. The retention of both local and long-range structures by the daughter $CfCl_3$ is expected in these $BkCl_3$ samples owing to the very small energies ($\leq$0.3 eV) imparted to the daughter Cf nuclei at the moment of β-particle emission ($E_{\beta^-} \leq 126$ keV) from the parent ^{249}Bk nucleus. These recoil energies are insufficient to remove the daughter Cf nucleus from the lattice site of its parent Bk nucleus, and thus the structure of the parent Bk compound is retained by the daughter Cf compound. These observations are in agreement with our earlier findings on dimorphic $BkBr_3$, where *o*-$CfBr_3$ resulted from the β decay of *o*-$BkBr_3$.[11]

Acknowledgment. We gratefully acknowledge the U.S. Department of Energy's Transplutonium Program Committee for making available the ^{249}Bk and ^{249}Cf used in this work as part of its national program of transplutonium element production and research.

Registry No. ^{249}Bk, 14900-25-5; ^{249}Cf, 15237-97-5; $^{249}BkCl_3$, 20063-16-5; $^{249}CfCl_3$, 89759-77-3.

(11) Young, J. P.; Haire, R. G.; Peterson, J. R.; Ensor, D. D.; Fellows, R. L. *Inorg. Chem.* **1980**, *19*, 2209.

Contribution from the Department of Chemistry, Texas A&M University, College Station, Texas 77843

Hydrothermal Synthesis of Copper Molybdates

Ahmad Moini, Roberta Peascoe, Philip R. Rudolf, and Abraham Clearfield*

Received April 11, 1986

Several copper molybdate phases were prepared either hydrothermally or by reflux reactions at ambient pressures. $Cu_4Mo_6O_{20}$ was obtained by the hydrothermal reaction of CuO and MoO_3 in H_2O. It is triclinic, space group $P\bar{1}$, with $a = 10.071$ (4) Å, $b = 9.796$ (6) Å, $c = 8.052$ (4) Å, $\alpha = 104.98$ (4)°, $\beta = 100.63$ (4)°, $\gamma = 82.91$ (4)°, and $Z = 2$. The structure consists of chains of edge-sharing MoO_6 octahedra with the copper ions residing between the chains. $Cu_3(MoO_4)_2(OH)_2$ was prepared through precipitation from the reaction of $CuSO_4 \cdot 5H_2O$ and $Na_2MoO_4 \cdot 2H_2O$. The same product formed hydrothermally when CuO and MoO_3 were treated in aqueous sodium molybdate. The use of NaOH in hydrothermal reaction led to the formation of $NaCu(OH)(MoO_4)$, which is isomorphous with the zinc phase previously reported. Hydrothermal treatment of $Cu_3(MoO_4)_2(OH)_2$ in sodium molybdate also resulted in the formation of the latter phase.

Introduction

The preparation and structure of a number of copper molybdate phases have been reported in the literature. Most of these phases were prepared by solid-state reactions of the oxides of copper and molybdenum. The first crystal structure determined was that of $CuMoO_4$ prepared at ambient pressures.[1,2] This triclinic phase and its isostructural analogue $ZnMoO_4$, were recognized as having more distorted structures compared to the similar phases formed with other 3d transition metals. The high-pressure form of $CuMoO_4$ has a triclinic (distorted wolframite) structure,[3] while some of the other high-pressure molybdates, e.g. $MnMoO_4$, are monoclinic.[4] One of the main structural features of both $CuMoO_4$ phases is the irregular coordination around copper, and in the low-pressure polymorph there is also the presence of different coordination numbers for individual copper atoms. This latter feature is also observed in the structure of $Cu_3Mo_2O_9$, which contains CuO_5 tetragonal pyramids in addition to distorted CuO_6 octahedra.[5] A partially reduced form of this compound[6] has a structure with the formula $Cu_{3.85}Mo_3O_{12}$ instead of $Cu_3Mo_2O_8$ as originally proposed.[7]

Studies on the phase relationships in the Cu_2O–CuO–MoO_3 system reveal the existence of two cuprous molybdates, $Cu_2Mo_3O_{10}$ and $Cu_6Mo_4O_{15}$.[8-11] Recently, the latter phase was described as $Cu_6Mo_5O_{18}$ rather than $Cu_6Mo_4O_{15}$.[12] The structure determination of this phase revealed a three-dimensional arrangement consisting of MoO_6 octahedra and CuO_4 tetrahedra. In addition to direct synthesis, these phases also form as the intermediate or final products in the reduction of cupric molybdates depending on the reaction temperatures. The temperature of preparation is a very important factor since each of the cupric or cuprous molybdates form only in a limited temperature range.

In addition to the interest that exists in the structural characteristics of transition-metal molybdates, their catalytic properties are also significant. $CuMoO_4$ has specifically been applied to the oxidation of propene.[13]

We report here the results of several reactions in aqueous media. The possibilities for forming new phases and growing crystals large enough for single-crystal X-ray studies were examined with use of both reflux and hydrothermal techniques. In this report we describe three such phases, namely $Cu_4Mo_6O_{20}$, $Cu_3(MoO_4)_2(OH)_2$, and $NaCu(OH)(MoO_4)$.

Experimental Section

All of the chemicals used were ACS reagent grade, and distilled, deionized water was used throughout.

Reflux Reactions. Several reactions were carried out with use of aqueous solutions of $Na_2MoO_4 \cdot 2H_2O$ and $CuSO_4 \cdot 5H_2O$ in the concentration range 0.5–1 M. One of the solutions was brought to boiling in a round-bottom flask. The second solution was added dropwise with stirring. The order of addition did not affect the nature of the final product. The mixture was refluxed for ca. 24 h. Similar procedures have been reported earlier.[14]

Hydrothermal Reactions. These reactions were performed in a small (15 mL) Parr bomb fitted with a Teflon liner. A typical reaction involved placing equimolar quantities of the solid starting materials, e.g. CuO and

* To whom correspondence should be addressed.

(1) Nassau, K.; Abrahams, S. C. *J. Cryst. Growth* **1968**, *2*, 136.
(2) Abrahams, S. C.; Bernstein, J. L.; Jamieson, P. B. *J. Chem. Phys.* **1968**, *48*, 2619.
(3) Sleight, A. W. *Mater. Res. Bull.* **1973**, *8*, 863.
(4) Sleight, A. W.; Chamberland, B. L. *Inorg. Chem.* **1968**, *7*, 1672.
(5) Kihlborg, L.; Norrestam, R.; Olivecrona, B. *Acta Crystallogr., Sect. B: Struct. Crystallogr. Cryst. Chem.* **1971**, *B27*, 2066.
(6) Katz, L.; Kasenally, A.; Kihlborg, L. *Acta Crystallogr. Sect. B: Struct. Crystallogr. Cryst. Chem.* **1971**, *B27*, 2071.
(7) Thomas, I. D.; Herzog, A.; McLachlan, D. *Acta Crystallogr.* **1956**, *9*, 316.
(8) Haber, T.; Machej, T.; Ungier, L.; Ziolkowski, J. *J. Solid State Chem.* **1978**, *25*, 207.
(9) Machej, T.; Ziolkowski, J. *J. Solid State Chem.* **1980**, *31*, 135.
(10) Machej, T.; Ziolkowski, J. *J. Solid State Chem.* **1980**, *31*, 145.
(11) Haber, J.; Jamröz, K. *J. Solid State Chem.* **1980**, *44*, 291.
(12) McCarron, E. M., III; Calabrese, J. C. *J. Solid State Chem.* **1986**, *62*, 64.
(13) Maggiore, R.; Galvagno, S.; Bart, J. C. J.; Giannetto, A.; Toscano, G. *Z. Phys. Chem. (Munich)* **1982**, *132*, 85.
(14) Clearfield, A.; Moini, A.; Rudolf, P. R. *Inorg. Chem.* **1985**, *24*, 4606.

0020-1669/86/1325-3782$01.50/0